

# Normal-metal hot-electron microbolometer with on-chip protection by tunnel junctions

D Chouvaev, L Kuzmin and M Tarasov

Department of Microelectronics and Nanoscience, Chalmers University of Technology,  
S-412 96 Gothenburg, Sweden

Received 22 June 1999

**Abstract.** We describe recent developments in a fully on-chip integrated antenna-coupled bolometer for astrophysical applications at millimetre and submillimetre wavelengths. We have developed a normal-metal hot-electron microbolometer with Andreev mirrors for thermal protection of the absorber and the coupling to the antenna. In previous experiments we could not operate the sensor at temperatures below 300 mK presumably because of the high external noise load. Our latest results with the absorber protected by tunnel junctions show how this problem can be solved experimentally. We have achieved noise performance mostly limited by the amplifier, which corresponds to expected detector NEP on the order of  $1.5 \times 10^{-17} \text{ W Hz}^{-1/2}$  at 100 mK.

## 1. Introduction

Cryogenic bolometers are the most sensitive direct detectors of infrared and millimetre wave radiation and are widely used for astronomical observations. Most common bolometers used in radio-astronomy are made with a suspended absorber, heated by incident radiation, and a semiconducting thermistor or are superconducting bolometers, where the sensor is a suspended chip with a superconducting structure [1, 2]. One disadvantage of existing bolometers is that they compromise sensitivity and speed: to reach  $\text{NEP} < 10^{-17} \text{ W Hz}^{-1/2}$  one needs to make the absorbing area large, which results in a large thermal capacity  $C$  and, consequently, a longer reaction time  $\tau = C/G$ , where  $G$  is thermal conductance between the absorber and environment. Another problem is that suspended structures are often fragile, and it is difficult to combine many of them into a 2D detector array.

The normal-metal hot-electron microbolometer (NHEB) with Andreev mirrors proposed in [3] and later partly implemented [4] holds promise. This is a planar microfabricated bolometer using an antenna to receive a signal (figure 1). In an antenna-coupled bolometer the sensor itself can be miniaturized, minimizing the thermal conductance. A microwave signal received by the antenna will induce current in a normal-metal resistor (absorber) and heat the resistor. This heat will be delivered first to the electron gas in the resistor. At temperatures below 0.5 K, the thermal coupling between electrons and phonons is very low, and the electrons will establish their own equilibrium at a temperature above the phonon temperature (hot-electron effect). In this sense, the electron gas in the resistor can be seen as a power absorber, and thermal conductance to the environment is limited by the energy exchange between

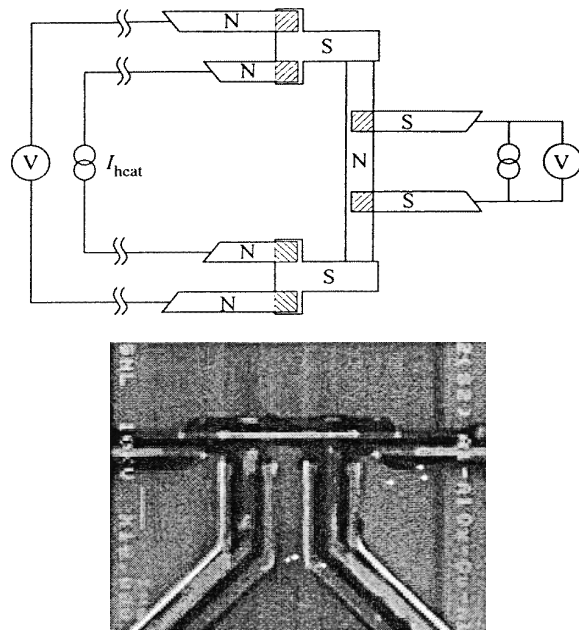


**Figure 1.** The bolometer schematic with additional NIS tunnel junctions in the absorber bias circuit for protection. Two NIS junctions in the measurement circuit are used to increase the response  $dV/dT$ . The SEM image shows a central part of the bolometer.

the electrons and the phonons. Thus one does not need to suspend the absorber to thermally isolate it. Furthermore, the thermal capacity of the electrons is much less than the thermal capacity of the whole structure, and this makes the sensor very fast.

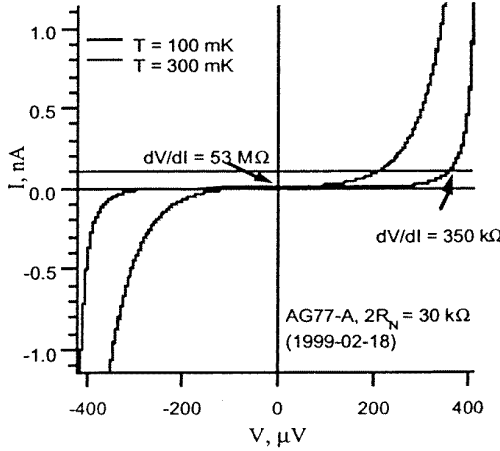


**Figure 2.** Principle of measuring electron temperature by means of two NIS tunnel junctions biased with constant current.

The authors of [3] suggest a very elegant solution for preventing the escape of heated electrons back to the antenna. They suggest using Andreev reflection [5] for thermal protection of the absorber while maintaining good electrical conductivity between the absorber and the superconducting antenna.

A small signal power results in a substantial rise of the electron temperature in the absorber. The temperature rise is converted to voltage response using one or two normal metal-insulator-superconductor (NIS) tunnel junctions, where the normal electrode is the absorber. When the junction is biased by fixed current, the voltage depends on the electron temperature in the N electrode (figure 2). The power responsivity of this sensor depends on temperature responsivity ( $dV/dT$ ) and heat conductance ( $G = dP/dT$ ):

$$S = \frac{dV}{dP} = \left| \frac{dV}{dT} \right| \left| \frac{dP}{dT} \right|^{-1}. \quad (1)$$

The temperature responsivity of the tunnel junctions is nearly constant across almost the whole range of operating temperatures (typically  $dV/dT \approx 3\text{--}5 \times 10^{-4} \text{ V K}^{-1}$ ). The heat conductance depends mostly on the properties of the absorber and can be estimated from the energy exchange rate between electrons and phonons in equilibrium at different temperatures [6]:

$$P = \Sigma \Omega (T_e^5 - T_p^5) \rightarrow \frac{dP}{dT} = 5 \Sigma \Omega T_e^4 \quad (2)$$

where  $\Omega$  is the absorber volume and  $\Sigma$  is a material parameter.

## 2. Device fabrication and measurement setup

The microbolometer is fabricated by e-beam lithography and shadow evaporation techniques. Three metal layers are used—a superconductor for NIS tunnel junctions (aluminium film, 36–38 nm), a normal metal for the absorber (copper, 58 nm), and a superconducting layer for the antenna (aluminium, 70 nm). The tunnel junctions are formed by oxidizing the first superconducting layer ( $P(\text{O}_2) = 0.3\text{--}0.4 \text{ mbar}$  and  $t = 0.5\text{--}2 \text{ min}$ ) resulting in the junction

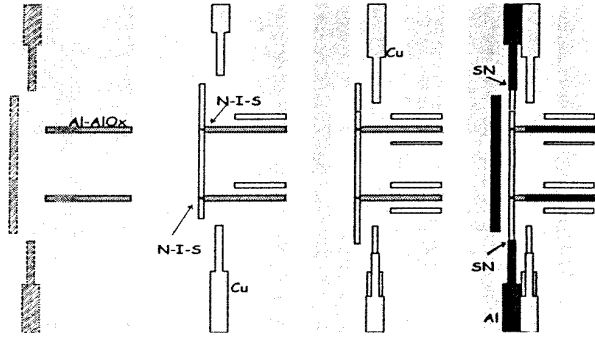


**Figure 3.** Schematic picture of the metal deposition process. A double PMMA copolymer resist is used to make a suspended mask. In the leftmost picture both resist layers are shown by slightly darker areas; the three other pictures show only the underlying copolymer mask. By tilting the sample in different planes the metal structures are shifted with respect to the original openings in the PMMA mask, providing necessary overlaps between subsequently deposited metal layers.

normal resistance of 5–15 kΩ for an area of about  $0.1 \mu \text{m}^2$ . The Andreev contacts between the absorber and the second superconductor can be made either by a two-step lithography process, with ion beam cleaning in between, or by our new single-step process which involves titling a sample in two perpendicular planes (figure 3). The dimensions of the copper absorber are  $4.5 \times 0.25 \mu\text{m}^2$ , the thickness is 58 nm and the resistance is about  $20 \Omega$ .

For dc measurements we have used a current bias for heating the absorber in a dilution refrigerator. The current sources for the NIS junctions and the absorber consist of symmetric voltage sources and two high-Ohmic (10 or 100 MΩ) resistors in series at room temperature. Johnson noise in those resistors is the main source of bias noise. For calibration measurements the voltage response from the tunnel junctions at the working bias is studied as a function of the bath temperature. I–V curves of the tunnel junctions at different bath temperatures are registered to determine the choice of working point. Then the sensor is tested by driving current through the absorber and measuring the response at a fixed cryostat temperature. Finally, noise spectra at different measurement conditions can be taken.

## 3. Experimental results

When we started our experiments, we obtained good power responsivity (at the predicted level) at relatively high electron temperatures above 300 mK but not in the temperature range 100–300 mK where it was most expected [7]. The reason for this was saturation of the response  $V(T)$  of the tunnel junctions, as can be seen in the calibration curves (figure 4).

Furthermore, the measured noise level was an order of magnitude higher than the noise of our amplifier, which was a modest  $30 \text{ nV Hz}^{-1/2}$  at 10 Hz. Later we realized that both these phenomena were related to intensive interference coupled to the absorber and heating the electrons sometimes to temperatures above 300 mK. The main clue convincing us of the validity of this hypothesis was a comparison of the voltage noise and the power responsivity of the device. Both dependences had very similar shapes, indicating that the noise

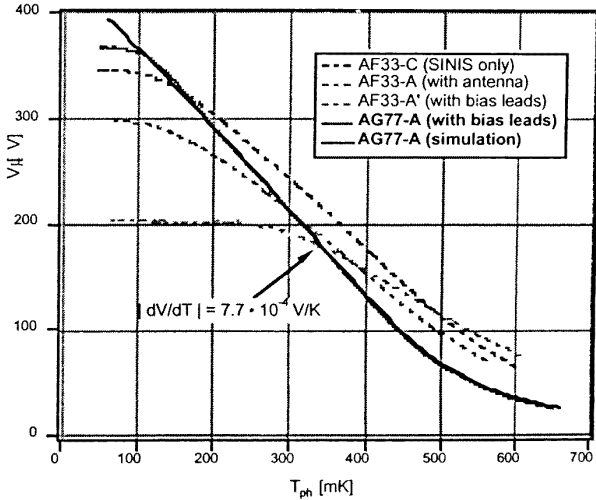


**Figure 4.** Comparison of  $V(T)$  dependences for different structures of non-protected sample AF33 (broken curves) and the same dependence for sample AG77, where additional tunnel junctions in the absorber bias leads have been used (the thick curve). A strong saturation can be seen for the structure with long bias leads on the sample AF33. Saturation is present even for the sample AG77, but only below 130 mK. The thin curve is a theoretical fit for this sample's  $V(T)$ .

was already present as fluctuations of electron temperature in the absorber.

Once convinced of the presence of external heating we tried to identify how the noise was getting in. Pick-up in the circuit connected for heating the absorber was one suggestion; microwave 'leakage' into the sample cavity was another. Since eliminating the latter would be a more difficult task, we started by breaking the absorber bias circuit using high-resistivity elements close to the absorber. We hoped that the voltage induced in the low-ohmic ( $R_{abs} = 20 \Omega$ ) circuit would drop in those high-resistivity links and thus not be able to generate any noticeable current. We chose NIS tunnel junctions on both sides of the absorber for these protecting links since they have very high intrinsic resistance in the sub-gap region and are very easy to fabricate simultaneously with other junctions (figure 1).

This measure has given surprisingly good results, bringing the  $V(T)$  saturation down to 100–130 mK (figure 4) and the noise level down almost to the amplifier level. However, the noise spectra (figure 5) show that connecting wires to the absorber and closing this circuit results in additional noise, thus indicating that even this strong protection is not perfect. Furthermore, even the noise associated with an isolated 'absorber' island ( $7\text{--}10 \text{ nV Hz}^{-1/2}$ ) is clearly higher than what is expected from the thermometry noise ( $3 \text{ nV Hz}^{-1/2}$ ). We think that some high-frequency leak still exists and is responsible for this additional noise.

The protection by tunnel junctions, however, completely distorted the heating power calibration at  $I_{absorber} > 0$ . Earlier we could assume that the dissipated power was  $P = P_J = R_{absorber} I_{absorber}^2$ . Now, as soon as  $I_{bias} > 0$  high-energy electrons are injected into the superconducting electrode of the protecting NIS junction as quasiparticles,

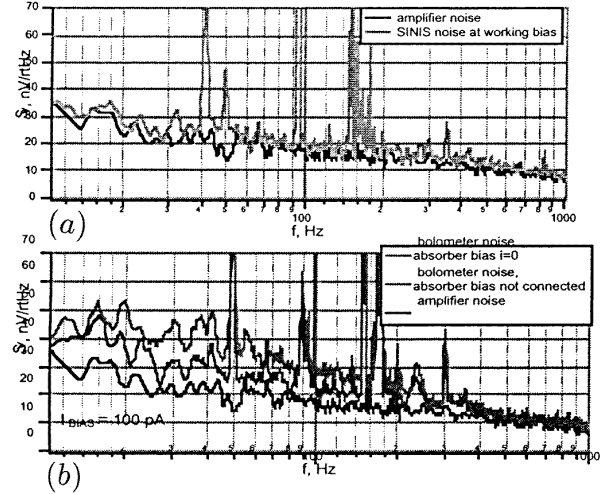


**Figure 5.** Noise spectra for (a) simple SINIS structure, i.e. without superconducting electrodes connected to the absorber, and (b) complete microcalorimeter structure equipped with protection NIS junctions and connected to long leads for biasing; the higher noise curve corresponds to leads terminated by a current source. The lowest curve in each graph is the amplifier noise.

they proceed to the absorber, where their energy apparently dissipates, giving  $P \gg P_J$ . This effect is similar to the electronic cooling by NIS tunnel junctions described elsewhere [8], but now our object is on the 'warm' side of the Peltier cooler. This is the reason why we could not directly measure the value of the power responsivity  $S$  at low temperature. We could only estimate  $S$  for the sample AG77 using formulae (1) and (2). For  $dV/dT \approx 3 \times 10^{-4} \text{ V K}^{-1}$  (figure 4),  $\Sigma \approx 3 \times 10^{-9} \text{ W } \mu\text{m}^{-3} \text{ K}^{-5}$  and  $\Omega = 0.065 \mu\text{m}^3$  one can obtain thermal conductance  $G = 1 \times 10^{-13} \text{ W K}^{-1}$  and power responsivity  $S = 3 \times 10^9 \text{ V W}^{-1}$  at 100 mK. Using this power responsivity and the measured output noise  $45 \text{ nV Hz}^{-1/2}$  at 10 Hz (figure 5) we can estimate the noise equivalent power  $\text{NEP} \approx 1.5 \times 10^{-17} \text{ W Hz}^{-1/2}$ .

Further modifications to the bolometer include reversing the NIS protecting junctions and thus setting the N part at the absorber side to solve the problem of overheating. Installing an additional NS interface between the superconducting electrodes going to the absorber and the N side of the protecting junctions would result in Andreev reflection that would interrupt the unwanted energy flow. Another simple (but probably not as elegant) solution is to use small external resistors bonded to the chip wiring.

The new results show that there are no severe problems with the sensor itself. If we manage to couple the absorber efficiently to an integrated antenna, and place the device in an enclosure with well-controlled input of high-frequency radiation, we expect it to function properly. Disregarding the input noise, the performance of the detector will be limited by thermal fluctuations in the absorber and the noise introduced by the electron temperature readout. The level of thermal fluctuations at a given operating temperature depends on the volume and material of the absorber.

#### 4. Conclusion

We have demonstrated a reasonable performance of the power sensor in an integrated antenna-coupled bolometer. We could operate it at temperatures down to 100 mK, where the responsivity of the sensor is much higher than in our earlier results (with effective temperature of the order of 300 mK). The measured noise level corresponds to  $\text{NEP} = 1.5 \times 10^{-17} \text{ W Hz}^{-1/2}$ , and it is dominated by input noise external to the sensor itself and the amplifier noise. Some refinement of the experiment is still needed to fully calibrate the device.

#### Acknowledgment

This work was supported in part by the Swedish SSF Foundation.

#### References

- [1] Richards P L 1994 *J. Appl. Phys.* **76** 1
- [2] Lee A T, Lee S-F, Gildemeister J M and Richards P L 1997 *Proc. 7th Int. Workshop on Low Temperature Detectors (Munich, July–August 1997)* pp 123–5
- [3] Nahum M, Richards P L and Mears C A 1993 *IEEE Trans. Appl. Supercond.* **3** 2124
- [4] Nahum M and Martinis J 1993 *Appl. Phys. Lett.* **63** 3075
- [5] Andreev A F 1964 *Sov. Phys.–JETP* **19** 1228
- [6] Wellstood F C, Urbina C and Clarke J 1989 *IEEE Trans. Magn.* **25** 1001
- [7] Chouvaev D, Kuzmin L, Tarasov M, Sundquist P, Willander M and Claeson T 1998 *Proc. 9th Int. Symp. On Space Terahertz Technology (Pasadena, March 1998)* p 331
- [8] Nahum M and Martinis J M 1994 *Appl. Phys. Lett.* **65** 3123